High resistive nanocrystalline Fe-M-O (M=Hf, Zr, rare-earth metals) soft magnetic films for high-frequency applications (invited)

doi: 10.1063/1.365498

High resistive nanocrystalline Fe-M-O (M=Hf, Zr, rare-earth metals) soft magnetic films for high-frequency applications (invited)

Y. Hayakawa and A. Makino
Central Research Laboratory, Alps Electric Co., Ltd., 1-3-5 Higashi-Takami, Nagaoka 940, Japan

H. Fujimori and A. Inoue
Institute for Materials Research, Tohoku University, 2-1-1 Katahira, Sendai 980-77, Japan

Microstructure, soft magnetic properties, and applications of high resistive Fe-M-O (M=Hf, Zr, rare-earth metals) were studied. The Fe-M-O films are composed of bcc nanograins and amorphous phases with larger amounts of M and O elements which chemically combine each other. Consequently, the amorphous phases have high electrical resistivity. The compositional dependence of magnetic properties, electrical resistivity, and structure have been almost clarified. For example, the high magnetization of 1.3 T, high permeability of 1400 at 100 MHz and the high electrical resistivity of 4.1 $\mu\Omega$ m are simultaneously obtained for as-deposited $Fe_{62}Hf_{11}O_{27}$ nanostructured film fabricated by rf reactive sputtering in a static magnetic field. Furthermore, Co addition to Fe-M-O films improves the frequency characteristics mainly by the increase in the crystalline anisotropy of the nanograins. The $Co_{44.3}Fe_{19.1}Hf_{14.5}O_{22.1}$ film exhibits the quality factor ($Q = \mu'/\mu''$) of 61 and the μ' of 170 at 100 MHz as well as the high Is of 1.1 T. This frequency characteristics is considered to be superior to the other films already reported. The films also exhibit high corrosion resistance in an isotonic sodium chloride solution. Therefore, these films enable us to realize the high-frequency magnetic devices, such as thin-film inductors and transformers for microswitching converters and ultrahigh-density recording heads. © *1997 American Institute of Physics.* [S0021-8979(97)56708-9]

I. INTRODUCTION

In recent years, rapid improvement and miniaturization have been in progress in electronic equipments. One of the key devices for miniaturization of small-sized electronic apparatuses, such as the portable communication tools or portable audio systems, is the magnetic components. For that aim, micromagnetic devices using thin-film inductors or transformers operating at high frequency have been proposed.[1] On the other hand, the capacity of data storage system for computers has been rapidly increased exceeding 1 Gbit/in.[2] using magnetoresistive reading heads. Such high-density recording requires high-frequency writing heads.

In order to realize those improvements in magnetic devices and parts, soft magnetic films with excellent frequency characteristics are strongly required as their core materials. Some studies have been tried to improve the frequency characteristics of soft magnetic films by multilayering, operating in the direction of magnetic hard axis with magnetization rotating mode and the increase in electrical resistivity (ρ)[2]. However, the film with sufficient frequency characteristics has not been obtained. Since 1993 we have found that $Fe_{55\text{-}82}M_{7\text{-}22}O_{10\text{-}34}$ (M=Hf, Zr, rare-earth)[3–5] nanostructured films exhibit the superior frequency characteristics to the soft magnetic films which have already reported. The Fe-M-O films are composed of fine-grained bcc phases below 10 nm in size and amorphous phases with larger amounts of M and O elements. And then, we have been trying to improve the frequency characteristics. In the present paper, we describe these results on the development of the films and their applications.

II. EXPERIMENTAL PROCEDURE

Fe-M-O films with 2–3 μm in thickness were deposited onto indirectly water-cooled glass substrates by an rf reactive sputtering technique in a mixed atmosphere of pure argon and oxygen. The deposition was performed in no magnetic field or a static magnetic field to induce in-plane uniaxial magnetic anisotropy. The composition of films was controlled with changing the number of pellets of M elements placed onto an pure-Fe or Fe-M alloy targets and by changing the oxygen flow ratio. Unless otherwise stated, the films presented in this paper are sputtered in no magnetic field.

Indirectly coupled rf plasma (ICP) atomic emission spectrometry or electron probe microanalysis were performed to determine the Fe and M contents of the films. The oxygen content was measured by inert-gas-fusion IR technique.

The films were subjected to annealing for 10.8 ks under a uniaxial magnetic field (uniaxial field annealing, UFA) of 160 kA/m at various temperatures in an evacuated atmosphere below 10^{-3} Pa.

The film structure was investigated by x-ray diffractometry using Co $K\alpha$ radiation and by field-emission-type 200 kV transmission electron microscopy (FE-TEM) combined with nanobeam electron diffraction and energy dispersive x-ray spectroscopy (EDX) using a beam diameter of 1 nm. The corrosion resistance was investigated by measuring the change of the magnetization of the samples before and after immersing in an isotonic sodium chloride solution.

Saturation magnetization (I_s) was measured by a vibrating sample magnetometer (VSM) under a magnetic field of 800 kA/m. Coercivity (H_c), magnetic anisotropy field (H_k), and the angle dispersion of magnetic anisotropy (a_{90})[6] were

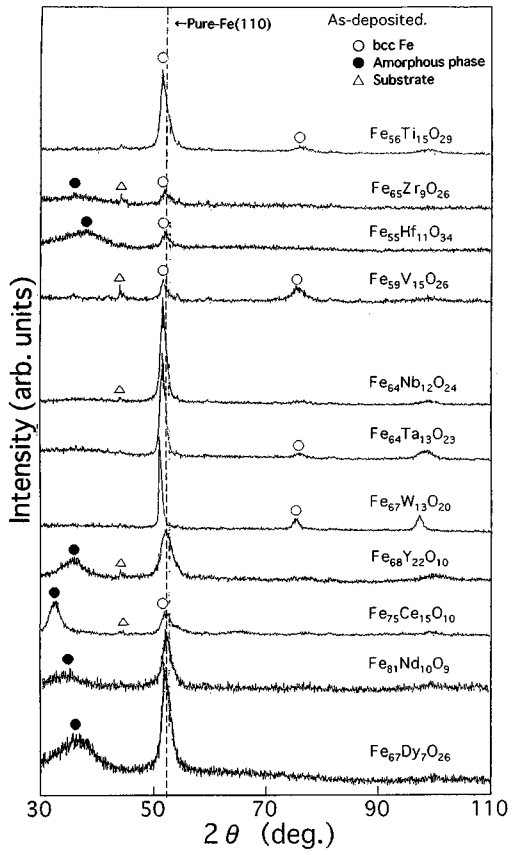

FIG. 1. X-ray diffraction patterns of as-deposited Fe-M-O films.

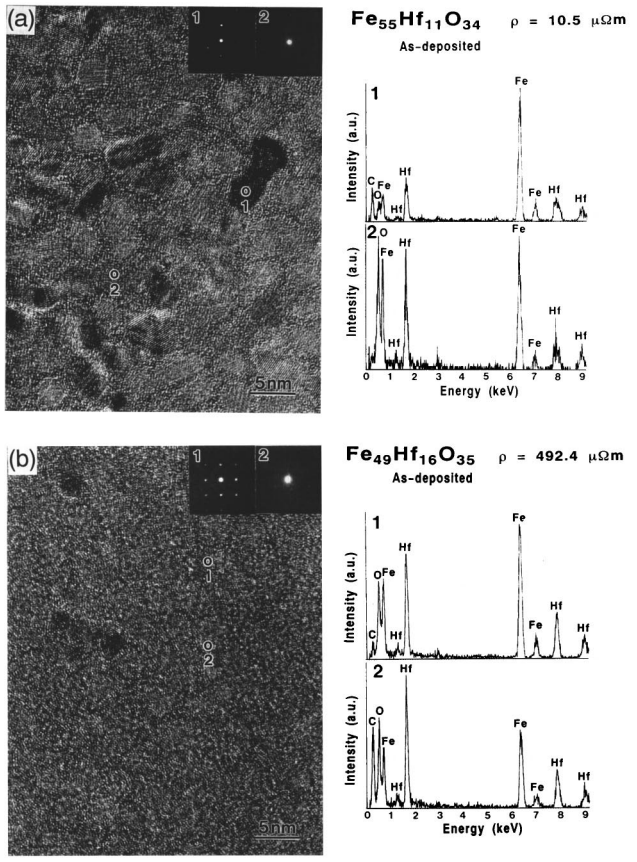

FIG. 2. High-resolution TEM images, electron diffraction patterns, and EDX spectra taken from each microregion for as-deposited (a) $Fe_{55}Hf_{11}O_{34}$ and (b) $Fe_{49}Hf_{16}O_{35}$ films.

determined by a dc *B-H* loop tracer. An optical cantilever method under an applied field of 4 kA/m was used for measuring saturation magnetostriction (λ_s). Permeability (μ', μ'') was measured by parallel line technique[7] under an applied field of 160 mA/m. Electrical resistivity (ρ) was measured by a four-probe method. All the measurements were carried out at room temperature.

III. RESULTS AND DISCUSSION

A. Microstructure and electrical resistivity

We have already reported[4] that the structure of as-deposited $Fe_{46-88}Hf_{2-22}O_{7-41}$ films determined from x-ray diffraction patterns is classified into four types, which consists of a single bcc phase, mixed bcc, and amorphous phases, a single amorphous phase, or oxide phases depending on the film composition. And soft magnetic properties are obtained in the films which have a bcc and an amorphous mixed structure. Figure 1 shows the x-ray diffraction patterns of as-deposited Fe-M-O (M=Ti, Zr, Hf, V, Nb, Ta, W, rare-earth metals) films. In M=Hf, Zr, and rare-earth systems which exhibit high ρ values, a broad peak originates from amorphous phase and a diffraction peak corresponding to bcc (110) are observed. On the contrary to these results, only the diffraction peaks corresponding to bcc phase are observed in M=Ti, V, Ta, Nb, W systems with larger amounts of M than those of Zr, Hf, and rare-earth and there is no halo in the x-ray diffraction patterns. Moreover, the diffraction angle of bcc (110) peaks shifts to lower angle side than that of pure-bcc Fe, indicated with a dashed line in the figure.

Figures 2(a) and 2(b) show high-resolution TEM (HR-TEM) images, nanobeam electron diffraction patterns, and EDX spectra for $Fe_{55}Hf_{11}O_{34}$ and $Fe_{49}Hf_{16}O_{35}$ films in the as-deposited state, respectively. The ρ values of both films are also shown in the figure. The electron diffraction patterns and the EDX spectra were taken from the points indicated in the figure. Both films are consisted of very fine-grained crystals less than 10 nm in diameter, which were surrounded by the amorphous phase. The grains with diameter less than 5 nm in size are smaller and the region of amorphous phase becomes larger for $Fe_{49}Hf_{16}O_{35}$ film than those for the $Fe_{55}Hf_{11}O_{34}$ film. These crystals are identified as bcc-Fe phase containing supersaturated Hf (and O) atoms from the nanobeam electron diffraction pattern and the EDX spectrum of the crystal (region 1). The ρ value increases from 10.5 up to 492.4 $\mu\Omega$ m with increase in the amorphous region of the film.

Figure 3 shows the XPS spectra of Fe $2p3/2$, Hf $4f7/2$, Y $3d5/2$, and Ta $4f7/2$ for as-deposited $Fe_{55}Hf_{11}O_{34}$, $Fe_{68}Y_{22}O_{10}$, and $Fe_{55}Ta_{18}O_{27}$ films. Each spectrum is indicated with filled triangle in the figure. In all systems, the binding energy of Fe 2p3/2 agrees with that of pure Fe. On the contrary, the binding energies of Hf $4f7/2$ and Y $3d5/2$ are close to those of HfO_2 and Y_2O_3, respectively. Therefore, O preferentially combines with Hf and Y in the $Fe_{55}Hf_{11}O_{34}$

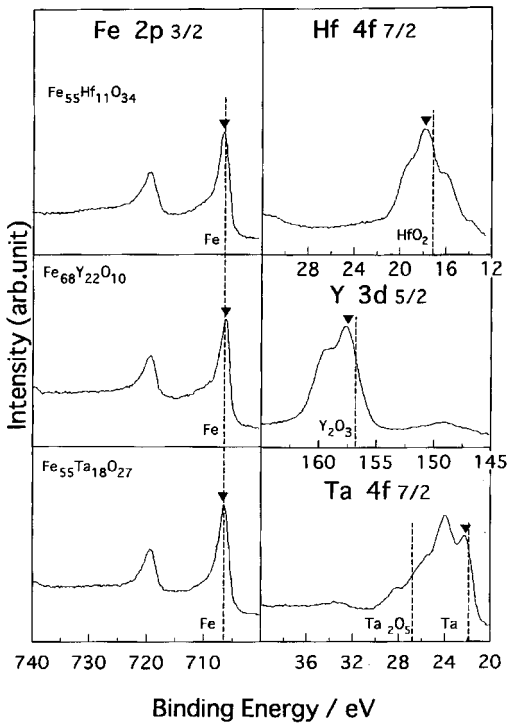

FIG. 3. XPS spectra for as-deposited $Fe_{55}Hf_{11}O_{34}$, $Fe_{68}Y_{22}O_{10}$ and $Fe_{55}Ta_{18}O_{27}$ films.

and $Fe_{68}Y_{22}O_{10}$ films which consist of bcc phase and amorphous phase, as shown in the Figs. 1 and 2. Then, those elements are mainly contained in the amorphous phase and they probably form M-oxide like structure. On the contrary, for $Fe_{55}Ta_{18}O_{27}$ film which consists of mostly single bcc phase, the binding energy of Ta $4f7/2$ is close to that of metallic Ta and there is no chemical binding between Ta and O elements. They are presumed to be supersaturated into the bcc phase, which results in the diffraction peak shift of bcc (110) as shown in Fig. 1. As a result, it is considered that the rapid increase in ρ results from the high resistive amorphous region for Fe-(Hf, Zr, rare-earth metals)-O films where M and O elements chemically combine.

B. Magnetic properties and applications

The compositional dependence of saturation magnetization (I_s) and coercivity (H_c) of as-deposited Fe-Hf-O films sputtered under no field are shown in Fig. 4. The symbols in the figure indicate film structure which was described before. Empty circles and solid circles indicate the single bcc phase and the single amorphous phase, respectively. Double circles indicate the oxide phase, and half solid circles represent the mixed phase of bcc and amorphous phase. The I_s has a tendency to decrease with increases in Hf and O contents and has a ridge around the Hf content of 10–15 at %. The H_c decreases with increases in Hf and O contents and has a valley around the same Hf content with the ridge of I_s. Therefore, the ridge of I_s approximately agrees with the valley of H_c, and there is a region in which I_s above 1.0 T and H_c below 160 A/m are simultaneously obtained. In this region, the real part of initial permeability (μ') exhibits about

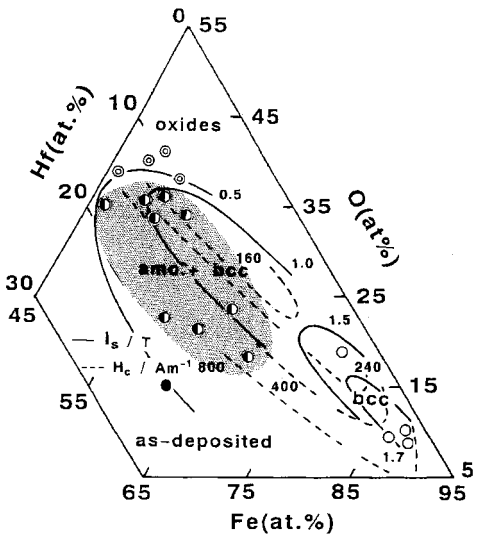

FIG. 4. Compositional dependences of saturation magnetization Is and coercivity H_c for as-deposited Fe-Hf-O films.

400 even in an as-deposited state,[4] and film structure is composed of fine bcc phase and amorphous phase (shaded).

Figure 5 shows the temperature dependence of I_s for as-deposited Fe-Hf-O films compared with a Fe-Hf amorphous alloy film. The Fe-Hf-O films which have the mixed structure of bcc and amorphous phase exhibit two-stage crystallization behavior.[4] The arrows put in the figure indicate the first crystallization temperature corresponding to the grain grows of bcc phases, which were measured by a differential scanning calorimeter. The I_s of both films decrease as a function of temperature with bending points in the course of changes, at 500 and 750 K for the $Fe_{49}Hf_{16}O_{35}$ and the $Fe_{55}Hf_{11}O_{34}$ film, respectively. An amorphous $Fe_{76}Hf_{24}$ film has a low Curie temperature (T_c) below room temperature owing to the Inver effect.[8] For a $Fe_{49}Hf_{16}O_{35}$ film, the bending point is considered to be resulted from the T_c of amorphous phase not from crystallization, because that temperature is lower than that of first crystallization. While, it is difficult to conclude obviously that the bending point is attributed to the T_c of amorphous phase for a $Fe_{55}Hf_{11}O_{34}$ film, because the temperature of the bending point is close to the

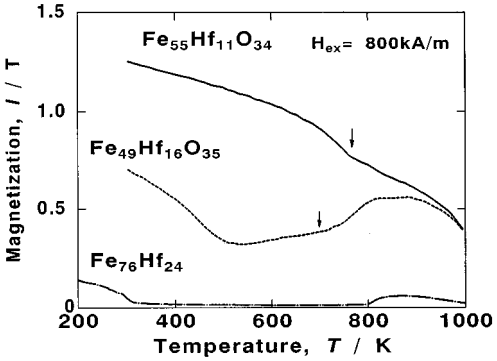

FIG. 5. Temperature dependence of saturation magnetization I_s for as-deposited $Fe_{76}Hf_{24}$, $Fe_{55}Hf_{11}O_{34}$ and $Fe_{49}Hf_{16}O_{35}$ film. The arrows indicate the first crystallization temperatures of Fe-Hf-O films.

TABLE I. Magnetic properties, electrical resistivity (ρ), and film structure for as-deposited Fe-M-O films.

	I_s(T)	H_c (Am^{-1})	ρ ($\mu\Omega$ m)	Structure
$Fe_{56}Ti_{15}O_{29}$	1.2	1040	6.4	bcc
$Fe_{65}Zr_9O_{26}$	1.3	211	6.6	amo.+bcc
$Fe_{55}Hf_{11}O_{34}$	1.2	154	9.1	amo.+bcc
$Fe_{59}V_{15}O_{26}$	1.2	···	5.6	bcc
$Fe_{64}Nb_{12}O_{24}$	1.3	168	4.1	amo.+bcc
$Fe_{64}Ta_{13}O_{23}$	1.3	658	4.7	bcc
$Fe_{67}W_{13}O_{20}$	1.3	···	8.3	bcc
$Fe_{68}Y_{22}O_{10}$	0.9	207	22.6	amo.+bcc
$Fe_{75}Ce_{15}O_{10}$	1.2	116	5.9	amo.+bcc
$Fe_{81}Nd_{10}O_9$	1.4	286	5.2	amo.+bcc
$Fe_{67}Dy_7O_{26}$	1.3	322	9.3	amo.+bcc

first crystallization temperature. However, there is no bending point below that temperature, and the T_c of amorphous phase for the $Fe_{55}Hf_{11}O_{34}$ film can be regarded as higher than 700 K. As a consequence, the T_c of amorphous phase including Fe and Hf increases by an addition of O in Fe-Hf-O films. Moreover, the T_c of amorphous phase for Fe-Hf-O films increased after annealing.[5] The magnetic properties, ρ values for as-deposited Fe-M-O (M=group IV A, V A elements and rare-earth metals) films are shown in Table I together with their film structure judged from the x-ray diffraction patterns and HR-TEM images. The film composition are equal to that of the films shown in Fig. 1. In all systems, I_s above 0.9 T and high ρ values above 4 $\mu\Omega$ m are simultaneously obtained. The values of saturation magnetostriction (λ_s) were $0.1-2.9\times10^{-6}$.[5] Relatively low H_c below 400 A/m is obtained in M=Hf, Zr, rare-earth metals systems, which have mixed structure of fine-grained bcc phases and amorphous phases.

In M=Ti, V, Ta, W systems, amorphous phases were not observed as shown in Fig. 1, H_c is relatively large and sufficient soft magnetic properties are not obtained. Therefore, to form the mixed structure composed of the fine-grained bcc phases and the amorphous phases is required to obtain the magnetic softness in an as-deposited state. The soft magnetic properties in as-deposited Fe-(Hf, Zr, rare-earth metals)-O films are probably resulted from the nanoscale grain size and the intergrain ferromagnetic coupling through the high-T_c amorphous phase as shown in Fig. 5, which averages out the magnetocrystalline anisotropy of bcc-Fe phase.[9] Moreover, it is possible to obtain the soft magnetic properties even in the films including rare-earth elements, which have a large magnetocrystalline anisotropy and usually inhibit soft magnetic properties, by weakening magnetic interaction between Fe and rare-earth elements which preferentially combine with O.

The soft magnetic properties of Fe-(Hf, Zr, rare-earth metals)-O films are improved by sputtering under an uniaxial magnetic field, or UFA treatment after deposition under no magnetic field. Furthermore, we tried to improve the frequency characteristics by enhancement of the uniaxial anisotropy (H_k) with addition of Co into the Fe-M-O films. Figure 6 shows the I-H curve for an as-deposited $Co_{44.3}Fe_{19.1}Hf_{14.5}O_{22.1}$ film compared with that of an

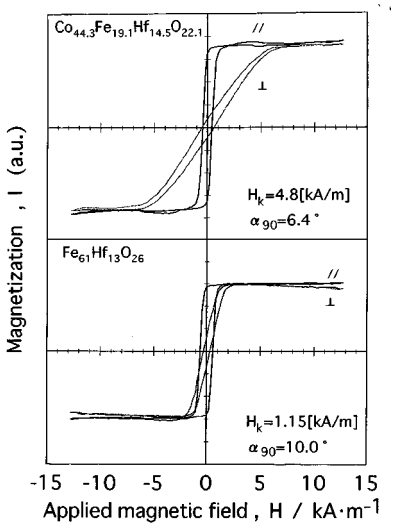

FIG. 6. Magnetization curves for an as-deposited $Co_{44.3}Fe_{19.2}Hf_{14.5}O_{22.1}$ film and an $Fe_{61}Hf_{13}O_{26}$ film after UFA at 673 K for 10.8 ks.

$Fe_{61}Hf_{13}O_{26}$ ternary alloy film. The former was deposited under a static magnetic field, the latter was UFA treated after deposition under no magnetic field. The H_k value of 1.15 kA/m for the $Fe_{61}Hf_{13}O_{26}$ film is largest in the all Fe-Hf-O films, however the H_k of the $Co_{44.3}Fe_{19.1}Hf_{14.5}O_{22.1}$ film exhibits 4.8 kA/m which is approximately four times larger than that of the $Fe_{61}Hf_{13}O_{26}$ film. This film shows the high Is of 1.1 T and high ρ value of 15.1 $\mu\Omega$ m simultaneously, and moreover, the angle dispersion of magnetic anisotropy becomes small. Therefore, excellent frequency characteristics are expected for the $Co_{44.3}Fe_{19.1}Hf_{14.5}O_{22.1}$ film owing to its significantly high ρ and large H_k values.

Figure 7 shows the frequency dependence of the μ, and quality factor ($Q=\mu'/\mu''$) of Fe-Hf-O films and a Co-Fe-Hf-O film fabricated by various methods, compared with other metallic soft magnetic alloy films which have ever been developed. The Q value is more important factor from a view point of applications. Actually, the conventional soft magnetic films exhibit high permeability at 1 MHz, in particular, approximately 10 000 is obtained for nanocrystalline soft magnetic films such as Fe-Si-Al-Hf-C film.[10] However, μ' decreases as a function of frequency because of their low ρ values. On the other hand, the μ' of Fe-Hf-O films is lower than that of conventional films up to around 30 MHz, while in the frequency range higher than that, Fe-Hf-O films exhibit higher and flat μ' characteristics over 100 MHz as a results of their high ρ values and moderate magnetic anisotropy field (H_k). The $Fe_{62}Hf_{17}O_{27}$ film shows the I_s of 1.3 T and high μ' value of 1400 at 100 MHz in an as-deposited state. Moreover, the Q values are also higher than that of conventional films. The highest Q value of 61 at 100 MHz is obtained for the $Co_{44.3}Fe_{19.1}Hf_{14.5}O_{22.1}$ film. Needless to say, these films have higher Q values than other metallic films even in low-frequency range. In the other M systems, similar frequency characteristics are observed, so that the Fe-M-O films and the Co-Fe-Hf-O film are considered to be low loss soft magnetic films in a wide frequency range from MHz to around GHz. In the figure, typical application items of the

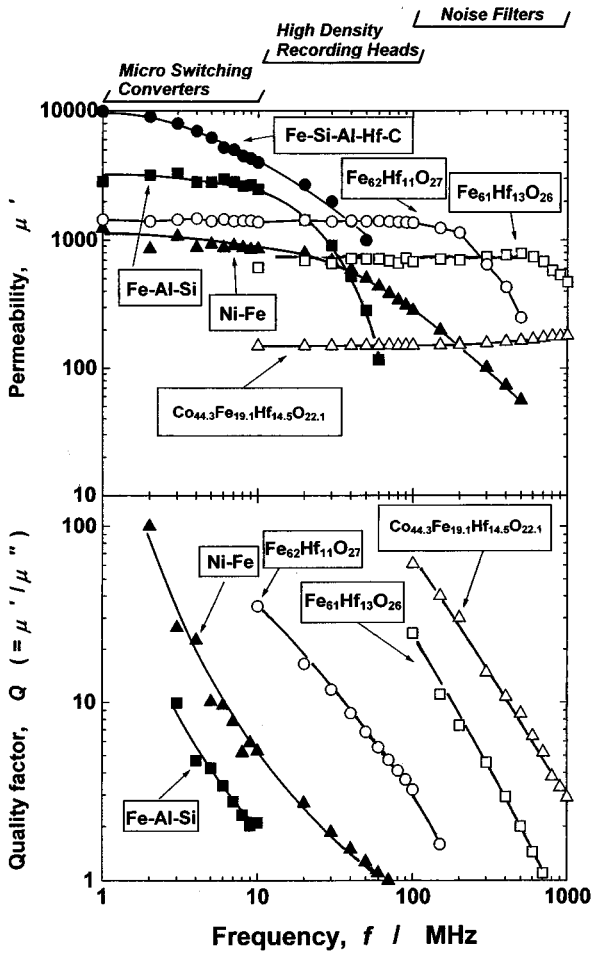

FIG. 7. Frequency dependence of the real part of initial permeability μ' and the quality factor $Q(=\mu'/\mu'')$ for an $Fe_{62}Hf_{11}O_{27}$ film (as-deposited), $Fe_{61}Hf_{13}O_{26}$ film (UFA) at 673 K for 10.8 ks, and $Co_{44.3}Fe_{19.1}Hf_{14.3}O_{22.1}$ film (as-deposited) compared with the other soft magnetic films have ever been reported.

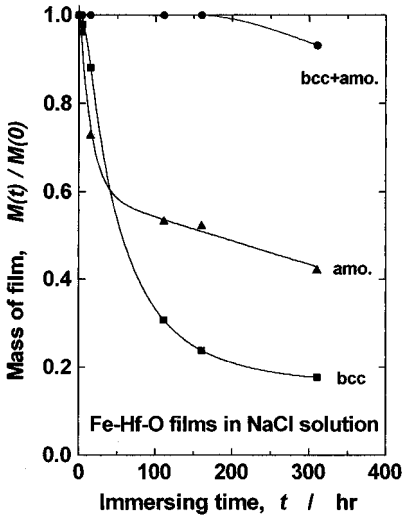

FIG. 8. Change in magnetization for as-deposited Fe-Hf-O films with various structure as a function of immersing time in NaCl solution.

Fe-M-O films and the Co-Fe-Hf-O film for each frequency range are also shown. In the frequency range around 10 MHz, we suppose the thin-film inductors or transformers for micro switching converters[11] for portable electric equipments. The microswitching dc-dc converters using Co-based amorphous alloy film as the core material of thin-film inductor have already been reported,[12,13] however, they will be operated at higher frequency for further miniaturization and improvement of power supplies. For such high-frequency switching converters operating around 10 MHz, the Fe-M-O films exhibit their ability as a core material.

Above those frequencies up to 100 MHz, Fe-M-O films are useful for magnetic heads for ultrahigh-density recording exceeding 1 Gbit/in^2. High B_s soft magnetic films such as Fe-Al-N[14] are studied for high-density recording heads, however, the high-frequency characteristics around 100 MHz must be required.

In the further high-frequency range around GHz noise filters, thin-film transformers[15] or other micromagnetic devices dealing electromagnetic waves will be proposed.

From a view point of application, high corrosion resistance is required to these films. We evaluated the corrosion resistance of Fe-Hf-O films by immersing in the isotonic sodium chloride (NaCl) solution. Figure 8 shows the changes in the mass of as-deposited Fe-Hf-O films evaluated from the magnetization as a function of immersing time in NaCl solution. The values of magnetization (emu) during the test are normalized by the value before immersing ($t=0$). In the figure, the film (a) has mixed structure consist of fine-grained bcc phase and amorphous phase, as shown in Fig. 2. The film structure of (b) and (c) are single bcc and amorphous phase, respectively. These structure were judged from x-ray diffraction patterns. There is no decrease in mass of the Fe-Hf-O film (a) after immersing for 150 h followed by a slight decrease after immersing for 300 h, and it exhibits high corrosion resistance in NaCl solution. On the contrary, the mass of Fe-Hf-O films (b) and (c) rapidly decrease, as film surfaces are covered with much rust. The high corrosion resistance of the Fe-Hf-O film [film (a)] is presumed to be corresponding to the high electrical resistive amorphous phase in which Hf and O elements chemically combine each other, and the bcc phase in which Hf and O elements are supersaturated. Also for the Co-Fe-Hf-O films, similar high corrosion resistance was observed. However, the details of the reason of these results have not been clarified in this study.

For an example of the applications, Figures 9(a) and 9(b) show a schematic illustration of a planar inductor for micro switching converters and the frequency dependence of $Q(=\omega L/R)$ values of a planer Cu coil using each magnetic films, respectively. The inductor is made up of a planar coil sandwiched with two magnetic films faced each other as shown in Fig. 9(a). In the case of the inductor, we use the one side of Cu coil as a conductor. As can be seen in Fig. 9(b), a inductor using Fe-Hf-O film shows a maximum. The Q value of 12.3 at 6 MHz and extremely high value of 21.8 at 20 MHz is obtained for a inductor using Co-Fe-Hf-O film. Therefore, these planar inductors using the Fe-Hf-O and Co-Fe-Hf-O films enables higher frequency operating and higher efficiency than the inductor using Co-Ta-Hf films for the

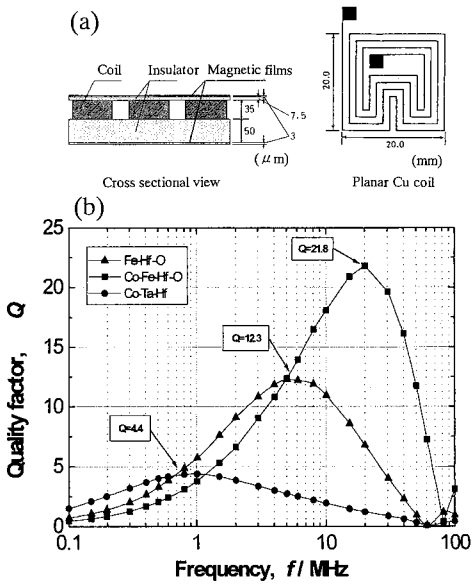

FIG. 9. Schematic illustration of planar inductor (a) and frequency dependence of quality factor $Q(=\omega L/R)$ of the inductor using Fe-Hf-O, Co-Fe-Hf-O, and Co-Ta-Hf amorphous films.

microswitching converters owing to the low loss characteristics of the magnetic films.

IV. CONCLUSIONS

The microstructure, the soft magnetic properties, and the applications of Fe-M-O (M=Hf, Zr, rare-earth metals) were described focusing on Fe-Hf-O and Co added films. The results obtained can be summarized as follows:

(1) The soft magnetic properties, I_s exceeding 0.9 T and H_c below 400 A/m, and high ρ values above 4 $\mu\Omega$ m are simultaneously obtained in as-deposited state. The structure of these films are composed of fine-grained bcc phases below 10 nm in diameter and amorphous phases in which larger amounts of M and O elements are included. O preferentially combines with M elements mainly in the amorphous phases. These films exhibit high corrosion resistance after immersing in NaCl solution for 300 h.

(2) By sputtering under an uniaxial magnetic field, I_s of 1.3 T and flat initial μ' of 1400 up to 100 MHz are obtained for a $Fe_{62}Hf_{11}O_{27}$ film in as-deposited state. By the addition of Co, the flat μ' of 170 up to 1 GHz and the highest Q of 61 at 100 MHz are obtained.

(3) The application of the Fe-M-O films and the Co-Fe-Hf-O film to magnetic devices are supposed depending on the operating frequency range as follows: 1–10 MHz: thin-film inductors and transformers for microswitching converters, 10–100 MHz: ultrahigh-density recording heads above 100 MHz: noise filters, other electromagnetic devices.

ACKNOWLEDGMENTS

The authors would like to thank Professor K. Yamasawa of Shinshu University for useful discussions on microswitching converters and Mr. K. Ohminato and Ms. K. Ohminato of Alps Electric Co., Ltd. for technical assistance of HR-TEM observations and experiments, respectively.

[1] K. I. Arai and M. Yamaguchi, J. Magn. Soc. Jpn. **17**, 642 (1993).
[2] H. Karamon, T. Masumoto, and Y. Makino, J. Appl. Phys. **57**, 3527 (1985).
[3] A. Makino and Y. Hayakawa, J. Jpn. Inst. Metall. **57**, 1301 (1993).
[4] A. Makino and Y. Hayakawa, Mater. Sci. Eng. A **A181/A182**, 1020 (1994).
[5] Y. Hayakawa and A. Makino, Nanostruct. Mater. **6**, 989 (1995).
[6] T. S. Crowther, J. Appl. Phys. **34**, 580 (1963).
[7] T. Kimura, M. Mitera, S. Terasaka, M. Nose, F. Matsumoto, H. Matsuki, H. Fujimori, and T. Masumoto, J. Magn. Soc. Jpn. **17**, 497 (1993).
[8] K. Fukamichi and H. Hiroyoshi, Sci. Rep. Res. Inst. Tohoku Univ. A **32**, 154 (1985).
[9] G. Herzer, IEEE Trans. Magn. **MAG-26**, 1397 (1990).
[10] N. Hasegawa, F. Koike, T. Konishi, T. Nakamura, and A. Nitta, Technical Report of IEICE, MR93-72, 1994.
[11] K. Yamasawa, K. Maruyama, I. Hirohama, and P. P. Biringer, IEEE Trans. Magn. **MAG-26**, 1204 (1990).
[12] T. Sato, A. Sawabe, T. Inoue, T. Mizoguchi, and M. Sahashi, IEEE Trans. Magn. **MAG-30**, 217 (1994).
[13] M. Mino, T. Yachi, A. Tago, K. Yanagisawa, and K. Sakakibara, IEEE Trans. Magn. **MAG-32**, 291 (1996).
[14] J. A. Bain, J. Wolfson, M. H. Kryder, Y. Yip, J. Reid, R. D. Silkensen, and R. H. Dee, IEEE Trans. Magn. **MAG-32**, 166 (1996).
[15] H. Tsujimoto and I. O, IEEE Trans. Magn. **MAG-31**, 4232 (1995).